RSC Advances

PAPER

View Article Online
View Journal | View Issue

Cite this: *RSC Adv.*, 2019, **9**, 42474

Methyl *N*-phenyl carbamate synthesis over Zn/Al/Ce mixed oxide derived from hydrotalcite-like precursors†

Min Kang,[a] Hai Zhou,*[a] Dajiang Tang,[a] Xiaomei Chen,[a] Ying Guo[a] and Ning Zhao*[b]

Received 19th November 2019
Accepted 16th December 2019

DOI: 10.1039/c9ra09642f

rsc.li/rsc-advances

Methyl *N*-phenyl carbamate (MPC) is an important intermediate for the green synthesis of methylene diphenyl diisocyanate (MDI) as well as many other important products. In the present work, Zn/Al/Ce mixed oxides derived from hydrotalcite-like precursors were employed as effective and recoverable heterogeneous catalyst for MPC synthesis *via* DMC aminolysis. Zn/Al/Ce hydrotalcite-like precursors prepared *via* coprecipitation method and the resulting catalysts were characterized by means of XRD, BET, SEM and XPS. Strong interactions within the Zn/Al/Ce mixed oxides were observed *via* the addition of appropriate amount of cerium. The mixed oxides containing 2.5% cerium showed high DMC aminolysis activity giving aniline conversion of 95.8%, MPC selectivity of 81.6% and MPC yield of 78.2%. Moreover, as a heterogeneous catalyst, it also exhibited superiorities of easy recovery and recyclable stability for MPC synthesis.

1 Introduction

Methyl *N*-phenyl carbamate (MPC) is a key intermediate that can be used for the synthesis of many important products, such as pesticides, pharmaceuticals, dyestuffs and so on.[1] More importantly, MPC can also be used for the green synthesis of methylene diphenyl diisocyanate (MDI), which is an important precursor for the synthesis of polyurethane (Scheme 1).[1–3] Traditionally, MDI is prepared industrially by using phosgene as one of the feedstocks, which could undoubtedly lead to serious environmental pollution and safety issues.[1] As a consequence, green synthesis of MPC is of great significance with respect to the non-phosgene synthesis of MDI and other isocyanates.

MPC could be synthesized *via* the reactions of phenylurea and dimethyl carbonate (DMC)[4] and/or methanol,[5] aniline and DMC[2,6–10] and/or methyl carbamate (MC),[3,11] and even aniline and C_1 source (*e.g.* CH_3OH and CO_2),[12–14] *etc.* And some new synthetic paths have also been developed recently. Among these synthetic procedures, the aminolysis of DMC for MPC synthesis is very attractive, because the byproducts methanol could be used for the production of DMC.[15] However, due to the high reactivity of the intermediates decomposed from DMC, carbamoylation and methylation proceed simultaneity during the aminolysis reaction, which, respectively, leads to the formation of MPC and *N*-methylaniline (NMA) and/or *N*,*N*′-dimethylaniline (DMA), as shown in Scheme 1.[2,16–18] Thus, developing catalysts with high activity is quiet necessary so as to enhance the selectivity as well as yield of MPC.

So far, various metal salts including Zn,[11,19–22] Pb,[8,11] Sn,[23] Na,[24] *etc.* had been successfully employed as homogeneous catalysts for the synthesis of MPC and other carbamates. Despite the high activity, these homogeneous catalysts also bring about troublesome problems such as products purification and catalysts recovery. In addition, $Zn(OAc)_2$ may dissolve and even gradually transform into ZnO, leading to decreased catalytic performance of $Zn(OAc)_2/SiO_2$ during repeatable use.[2] Thus, the development of heterogeneous catalysts for the synthesis of carbamates is very attractive. Recently, CeO_2,[16,25–30] Au/CeO_2,[31] MnO_x–CeO_2,[32] TiO_2–Cr_2O_3/SiO_2,[33] ZnO–MgO,[34] and zinc alkyl carboxylate covalently bonded on silica,[6] *etc.* have been developed as heterogeneous catalysts for the synthesis of carbamates. And substantial improvements have been achieved in the aspects of reactivity, selectivity, stability as well as the reaction mechanism. Laursen *et al.* investigated the dissociation process of DMC on CeO_2 *via* first-principles calculation, which showed that the selectivity of CeO_2 toward carbamoylation strongly depend on its crystal shape, and CeO_2 nano-octahedra exposing (111) facets was more active and selective than CeO_2 nano-rods and nano-cubes.[16] Zinc alkyl carboxylate

[a]*Department of Chemistry and Chemical Engineering, Zunyi Normal College, Zunyi 563002, China. E-mail: 591658314@163.com; Fax: +86-851-28924799; Tel: +86-851-28924799*

[b]*State Key Laboratory of Coal Conversion, Institute of Coal Chemistry, Chinese Academy of Sciences, Taiyuan 030001, China. E-mail: Zhaoning@sxicc.ac.cn; Fax: +86-351-4041153; Tel: +86-351-4063121*

† Electronic supplementary information (ESI) available: XPS of Zn 2p, Al 2p and Ce 3d core-level of catalysts, results of the optimization of reaction conditions, and the SEM image of Zn/Al/Ce2.5 after 5 times cyclic test. See DOI: 10.1039/c9ra09642f

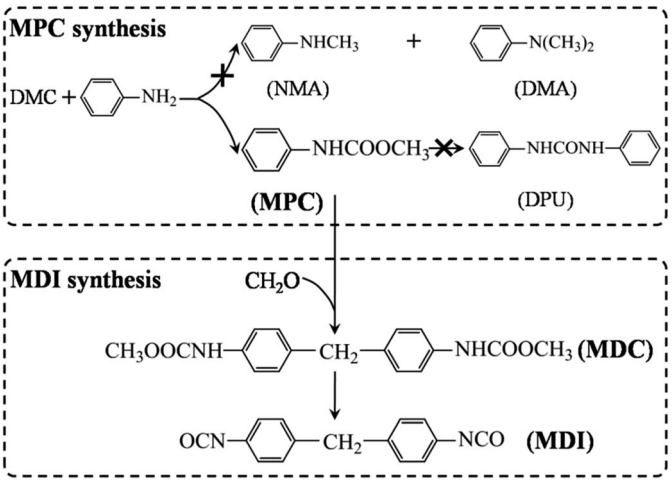

Scheme 1 The possible reaction paths of DMC aminolysis and MDI synthesis using MPC as feedstock. The symbol "×" shows the unselective byproducts of DMC aminolysis.

covalently bonded on silica could show almost unchanged activity during repeated evaluation for 12 times under a moderate conversion of aniline.[6]

It is widely reported that hydrotalcite-like compounds (HTlcs) are excellent precursors for preparing mixed oxides catalysts, because catalysts derived from calcined HTlcs possess superior properties of high dispersion of metallic active sites and unique surface acid–base properties.[35–38] Thus, considering the fact that metal cations in HTlcs are highly adjustable, and zinc and cerium are two of the main active components, herein, we demonstrate the design and fabrication of Zn/Al/Ce mixed oxides derived from calcined Zn/Al/Ce HTlcs precursors for MPC synthesis *via* DMC aminolysis. The results show that Zn/Al/Ce mixed oxides possessing 2.5% cerium is highly active and stable, giving aniline conversion of 95.8%, MPC selectivity of 81.6% and MPC yield of 78.2%.

2 Experimental

2.1 Catalysts preparation

All the regents were of analytic grade and used without further purification. A series of HTlcs with Zn–Al–Ce atomic ratio of $75:25-x:x$ ($Zn^{2+}:(Al^{3+}+Ce^{3+})=3:1$) were prepared *via* coprecipitation method, where x was equal to 0, 1, 2.5, 5, 7.5 and 10. The typical preparation process of HTlcs was as follows: calculated amount of $Zn(NO_3)_2\cdot 6H_2O$, $Al(NO_3)_3\cdot 9H_2O$ and $Ce(NO_3)_3\cdot 6H_2O$ were dissolved in distilled water, forming solution A. Then NaOH and Na_2CO_3 with the molar ratio of 3 were dissolved in distilled water, forming solution B. Solutions A and B were added dropwise into another baker that contained 100 mL distilled water under vigorous stirring. During coprecipitation, the pH of solution was maintained at 10 ± 0.5. After aged for 24 h at 80 °C, the suspension was filtered and washed several times with distilled water. The filter cake was dried at 80 °C and calcined at 500 °C for 4 h. The resulting catalysts with the above mentioned compositions were denoted as Zn/Al/Ce0, Zn/Al/Ce1, Zn/Al/Ce2.5, Zn/Al/Ce5, Zn/Al/Ce7.5 and Zn/Al/Ce10, respectively.

2.2 Characterization

The precursors and catalysts were characterized by X-ray diffraction (XRD) on a Rigaku D/max-rB diffractometer with Cu Kα radiation. Scanning electron microscopic (SEM, Scios, FEI) was used for observing the morphology of samples at acceleration voltages of 20 kV. Nitrogen adsorption–desorption properties of the samples were measured on Quantachrome Autosorb-IQ2-MP-XR-VP at 77 K, the specific surface area was obtained *via* Brunauer–Emmett–Teller (BET) method from the N_2 adsorption–desorption isotherms. X-ray photoelectron spectroscopy (XPS) data was collected on an ESCALAB250Xi spectrometer (Thermo Fisher Scientific). All the binding energies were calibrated internally by adventitious carbon deposit C 1s peak at 284.8 eV. The Thermo Avantage software was used to analyze the XPS data.

2.3 Catalytic evaluation

MPC synthesis was carried out in a 50 mL Teflon-lined autoclave equipped with a magnetic stirrer. In a typical experiment, 19.35 g DMC, 0.8 g aniline (the molar ratio of DMC to aniline was 25) and 0.253 g catalyst were added into the reactor. Under a nitrogen atmosphere, the reaction proceeded at 200 °C for 7 h. After reaction, the catalyst was separated by centrifugation and the liquid product was analyzed by high performance liquid chromatography (HPLC).

Shimadzu LC-20A HPLC equipped a Shimadzu C-18 (4.6 mm × 150 mm, 5 μm) column was used to analyze the liquid product. The mobile phase was CH_3OH/H_2O (70/30, volume-to-volume), the flow rate of mobile phase is 0.4 mL min^{-1}. The column temperature was 40 °C, and the detection wavelength was 254 nm.

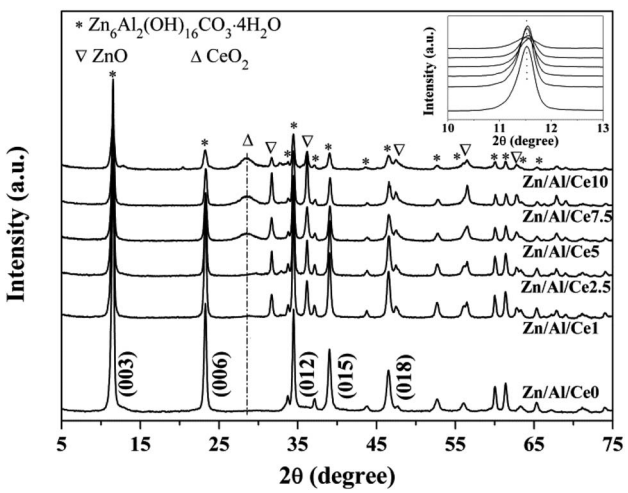

Fig. 1 XRD patterns of the uncalcined Zn/Al/Ce HTlcs precursors.

3 Results and discussion

3.1 Characterization

XRD patterns of uncalcined Zn/Al/Ce precursors are displayed in Fig. 1. Apparently, all samples show a series of strong diffraction peaks at *ca.* 11.6, 23.3, 34.4, 39.1 and 46.5°, corresponding to $Zn_6Al_2(OH)_{16}CO_3 \cdot 4H_2O$ crystal facets of (003), (006), (012), (015) and (018), respectively. This suggests that the as-prepared precursors show the typical characteristics of Zn/Al HTlcs (JCPDS: 38-0486). In accordance with previous literatures, the peak intensities of the Ce-containing samples decrease with the increase of cerium content, revealing the decreased crystallinity.[35–37] No apparent diffraction peaks shift could be observed over the Ce-containing samples (the inset of Fig. 1), as compared with pure Zn/Al HTlcs. Even though, the XRD results still suggest that the addition of cerium significantly affect the formation process of the as-prepared Zn/Al HTlcs precursors (*e.g.* structure distortion and low crystallinity), due to the larger ionic radius of Ce^{3+} (0.101 nm) as compared with that of Al^{3+} (0.054 nm).[36] Meanwhile, previous report also proved that high Zn^{2+}/Al^{3+} ratio would result in deformation of the layered structure,[37] which was not favor the formation of HTlcs. As for the present study, the content of aluminum decreases with the increase of cerium, the low aluminum content would also lead to the decrease of HTlcs phase. As a result, besides the Zn/Al HTlcs as the dominate phase, trace amount of ZnO (JCPDS: 36-1451) can also be observed owing to the decreased crystallinity and the relative high aging temperature (80 °C).[37] Similarly, the diffraction peak at 28.6° may suggest that a portion of cerium transforms into CeO_2 (JCPDS: 34-0394) after the aging process.

The precursors are then calcined at 500 °C for 4 h, so as to ensure the obtained catalysts possessing relative high specific area and strong interactions within the mixed oxides.[35,36] The XRD patterns of the resulting Zn/Al/Ce catalysts are presented in Fig. 2. After calcination, the Zn/Al HTlcs phase disappears and transforms into mixed oxide phases, which include the species of ZnO (JCPDS: 36-1451) and CeO_2 (JCPDS: 34-0394). Apparently, the diffraction peaks of CeO_2 increases with the increase amount of cerium, which indicates the high crystallinity and agglomeration of CeO_2 at high cerium content. Moreover, as for the Ce-containing catalysts, the diffraction peaks of ZnO (101) facet located at *ca.* 36.5° shift toward lower angles (the inset of Fig. 2), which may be caused by the incorporation Ce^{4+} cations with larger ionic radius.[36] No crystalline Al_2O_3 can be observed in all the XRD patterns, indicating that aluminum oxide mainly exists in the form of amorphous phase.

In order to investigate the interactions between the different oxides within the Zn/Al/Ce catalysts, they are characterized by means of XPS. It is found that both the binding energy of Zn 2p and Al 2p shift toward higher binding energy after the introduction of cerium. And catalysts with relative low cerium content (*e.g.* Zn/Al/Ce1 and Zn/Al/Ce2.5) exhibit larger shift than the rest three Ce-containing catalysts, as shown in Fig. S1 and S2.† Correspondingly, the binding energy of Ce 3d for Zn/Al/Ce1 and Zn/Al/Ce2.5 shift toward lower binding energy as compared to Zn/Al/Ce2.5, Zn/Al/Ce7.5 and Zn/Al/Ce10 (Fig. S3†). Fig. 3 shows the high resolution XPS spectra of Ce 3d. According to literatures, it can be deconvoluted into eight peaks corresponding to Ce $3d_{3/2}$ and $3d_{5/2}$.[39,40] The peaks located at *ca.* 885.2 and 903.4 eV suggest the presence of Ce^{3+}, and the rest peaks located at *ca.* 882.1, 888.4, 898, 900.6, 907.2 and 916.4 eV can be assigned to Ce^{4+}. The amount of Ce^{3+} could be calculated according to the relative contribution of Ce^{3+} features to the spectrum. As displayed in Table 1, the ratio of Ce^{3+}/Ce^{4+} almost increases with the decrease of cerium content within the Zn/Al/Ce mixed oxides, and Zn/Al/Ce2.5 possesses the highest Ce^{3+}, which is somewhat in accordance with the binding energy shift of Zn 2p and Al 2p. It should be mentioned that the identification of Ce^{3+} is just simplification since it only corresponds to the center of most intense peak for Ce_2O_3.[40] Eve though, it could still reflect the surface electron rich state of CeO_2 within the

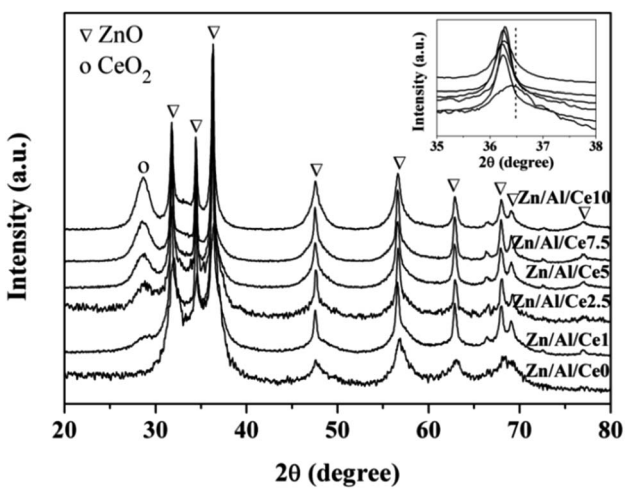

Fig. 2 XRD patterns of the Zn/Al/Ce catalysts.

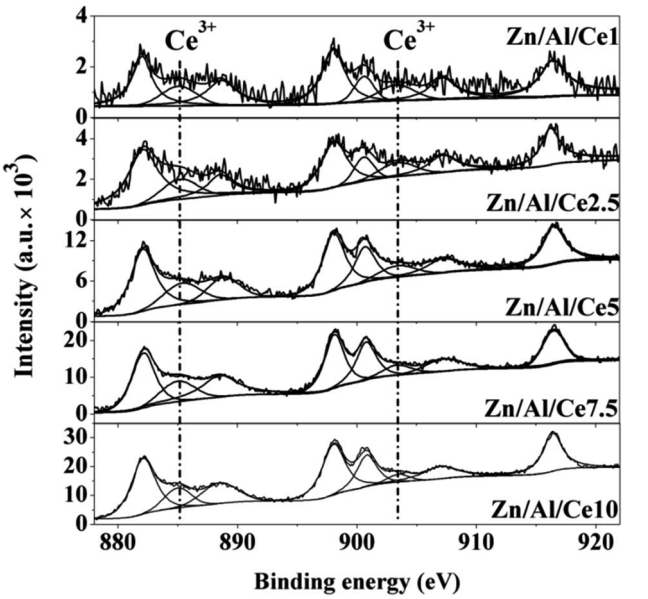

Fig. 3 XPS of Ce 3d core-level of the Zn/Al/Ce catalysts.

Table 1 Physicochemical properties of the resulting Zn/Al/Ce catalysts

Catalysts	SSA ($m^2\ g^{-1}$)	Average pore size (nm)	[a]Atomic ratio (%)			
			Zn	Al	Ce	[a]Ce^{3+}/Ce^{4+}
Zn/Al/Ce0	44.1	7.6	80.3	19.7	0	
Zn/Al/Ce1	35.3	8.2	79.3	19.8	0.8	14.86%
Zn/Al/Ce2.5	31.3	8.9	79.2	19.0	1.8	15.10%
Zn/Al/Ce5	40.2	9.6	76.0	20.0	3.9	14.53%
Zn/Al/Ce7.5	29.8	9.3	75.8	17.6	6.6	13.96%
Zn/Al/Ce10	43.5	10.8	76.4	14.8	8.8	11.08%

[a] The atomic ratio and the ratio of Ce^{3+}/Ce^{4+} are determined by XPS results.

mixed oxides, which suggests the transferring of electron from zinc and aluminum atoms to cerium atoms, especially for Zn/Al/Ce1 and Zn/Al/Ce2.5.

SEM images of the HTlcs precursors are shown in Fig. S4.† In accordance with literatures,[36,37] all the precursors exhibit nanoplates structure with the diameter of several hundred nanometers. The size of the nanoplates increases with the increasing of cerium content. It further confirms the influence of cerium on the formation of Zn/Al/Ce HTlcs, which is in accordance with the XRD results. The SEM images of the resulting Zn/Al/Ce catalysts are presented in Fig. 4. As can be seen, Zn/Al/Ce catalysts still keep the nanoplates structure, and the decreased size of the catalysts suggests the shrinkage and fraction of the nanoplates during the thermal decomposition of basic carbonate precursor. Similar with the precursors, the Zn/Al/Ce catalysts with higher cerium content still possess larger size. The specific surface area (SSA) of Zn/Al/Ce catalysts is in the range of 30–45 $m^2\ g^{-1}$, and no regular changes in SSA could be drawn due to the low values, as shown in Table 1. However, the average pore size of the catalysts increases with the increasing of cerium content, which may result from the decomposition of Zn/Al/Ce HTlcs precursors with high distortion and low crystallinity.

3.2 Catalytic performance

The above results suggest that the addition of cerium have remarkable influence on the phase, microstructure and even chemical state of Zn/Al/Ce precursors as well as the resulting catalysts. Accordingly, strong interactions between the Zn/Al/Ce mixed oxides within the resulting solid catalysts are expected. As a result, reaction conditions of reaction temperature, reactant molar ratio and reaction time are optimized over Zn/Al/Ce2.5.

As for DMC aminolysis, carbamoylation and methylation are the two main reactions, which are strongly affected by reaction temperatures.[2,16–18] It was generally reported that incorrect increasing of reaction temperature could enhance methylation, resulting in a decrease of MPC selectivity. Thus, reaction temperature is optimized firstly (the molar ratio of DMC to aniline is 20, and reaction time is 7 h, Fig. S5†). The conversion of aniline increases sharply with the increase of temperature from 150 to 210 °C. The selectivity and yield of MPC increase with the increasing of temperature, reach the maximum value of 66.4% and 60.4%, respectively, at 200 °C. Afterwards, both the selectivity and yield of MPC decrease sharply, which is probably caused by the methylation of aniline at elevated temperature.[2,6,19] Subsequently, the molar ratio of DMC to aniline is also optimized, as shown in Fig. S6.† It should be

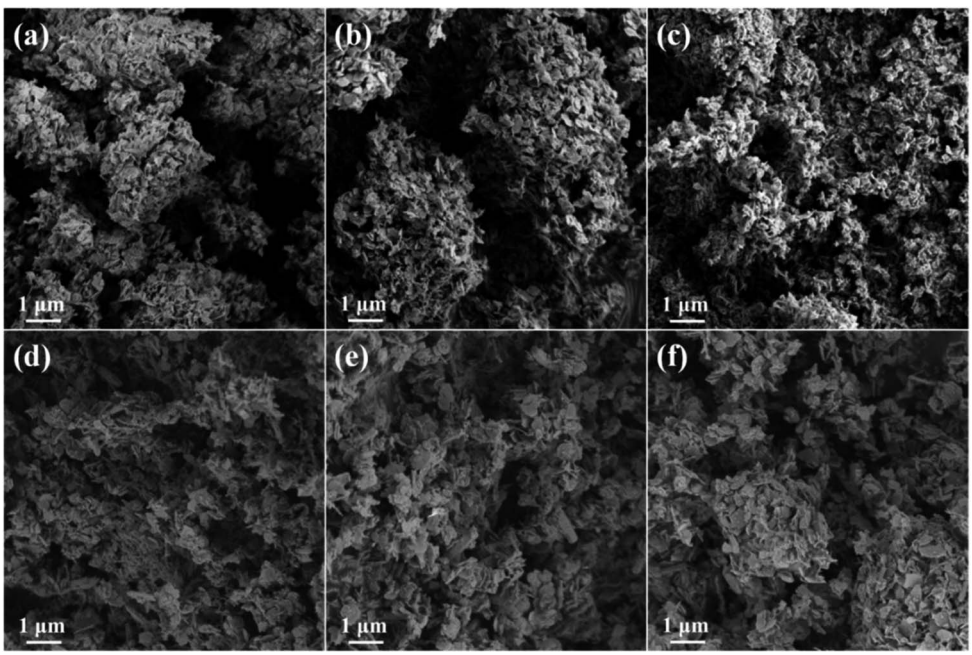

Fig. 4 SEM images of the resulting catalysts (a) Zn/Al/Ce0, (b) Zn/Al/Ce1, (c) Zn/Al/Ce2.5, (d) Zn/Al/Ce5, (e) Zn/Al/Ce7.5 and (f) Zn/Al/Ce10.

mentioned that the catalytic performance enhances when the molar ratio of DMC to aniline increases to 25, giving aniline conversion of 95.8%, MPC selectivity of 81.6% and MPC yield of 78.2%. It is reported that DMC acts as solvent and reactant during DMC aminolysis reaction.[19] Thus, excessive DMC would promote the conversion of aniline as well as the selectivity of MPC by suppressing the side reactions. The influence of reaction time is further investigated (Fig. S7†). The conversion of aniline increases with the increasing of reaction time, reaching *ca.* 95% at 5 h and remaining unchanged with further increase of reaction time. The maximal selectivity and yield of MPC are obtained at 7 h and then decrease sharply. As a result, the chosen reaction time is 7 h.

Table 2 displays the catalytic performance over the series of Zn/Al/Ce catalysts with different cerium content under the optimized reaction conditions. As can be seen, without the addition of cerium Zn/Al/Ce0 shows a certain catalytic activity, the aniline conversion is 91.0%, MPC selectivity is 63.3% and the MPC yield is 57.6%. The activity of Zn/Al/Ce0 might originate from the surface acidic sites of Zn/Al mixed oxide[38] as well as zinc element that is generally used as the active component for carbamates synthesis.[2,6,22,41] Nevertheless, methylation proceeds obviously, giving the NMA and DMA selectivity of 10.9% and 24.3%, respectively. Aniline conversion, MPC selectivity and MPC yield increase over the Ce-containing Zn/Al/Ce catalysts, among which Zn/Al/Ce2.5 shows the highest carbamoylation catalytic activity. Both the selectivity and yield of MPC decrease gradually with the further increasing of cerium content, while the selectivity of methylation byproducts enhances apparently. As a consequence, the catalytic performance of Zn/Al/Ce10 is very close to that of Zn/Al/Ce0.

The above results suggest that high performance heterogeneous catalysts could be obtained *via* the addition of appropriate amount of cerium into Zn/Al mixed oxides. As evidenced by XPS, Zn/Al/Ce2.5 possesses the highest Ce^{3+} fraction owing to the strong interactions within the mixed oxides. Thus, it can be deduced that a proper interactions between Ce^{3+} of this solid catalysts and DMC would be generated, which would then result in higher catalytic activity for MPC synthesis.[34,38] However, high agglomeration of CeO_2 is expected under high cerium content, which leads to the nonuniform dispersion of metallic elements as well as the increased surface Ce^{4+} sites. And CeO_2 particles enclosed by unfavorable low energy facets (*e.g.* (100)) may also form.[16,30,42] The above two aspects may promote the unselective dissociation of DMC, leading to the increased selectivity of NMA and DMA. As a result, the catalytic performance of Zn/Al/Ce2.5, Zn/Al/Ce5 and Zn/Al/Ce7.5 decrease gradually, suggesting the adverse influence of cerium under high content. Moreover, it should be mentioned that high cerium content is benefit for the formation of larger pore size (Table 1), and the surface acid–base sites might be more effectively turned with the addition of relative larger amount of cerium, thus Zn/Al/Ce5 and Zn/Al/Ce7.5 possess than Zn/Al/Ce1. Consequently, MPC synthesis over the present Zn/Al/Ce heterogeneous catalyst is affected by many factors, such as Ce^{3+} fraction, SSA, pore size, surface acid–base sites and so on. And much work is needed before clearly discerning the activation mechanism of DMC and/or amine over this kind of heterogeneous catalyst.

Properties of the stability and recyclability of heterogeneous catalysts is crucial for industrial application. In this study, the cycling stability of Zn/Al/Ce2.5 was also investigated, which was conducted as follows: after each reaction, the solid catalyst was collected by centrifugation, washed with methanol under ultrasonic for several times and dried at 60 °C for 12 h. Because some catalyst was lost during the recovery process, a certain amount of fresh catalyst (*ca.* 20%) was added so as to ensure the mass of catalyst (0.253 g) in the reaction system unchanged. The results are shown in Fig. 5. To our delight, the conversion of aniline is kept at about 95%, and MPC selectivity and yield decrease very slowly during the 5 repeated times. The selectivity of the main methylation byproducts (DMA) is 13.3% in the first use, which gradually increases to 24.6% after the fifth cycles, while selectivity of NMA and DPU remain at *ca.* 4% and 0.6%, respectively. The MPC selectivity and yield are found to be 68.6% and 65.2%, respectively, after 5 cycles. As shown in Fig. S8,† Zn/Al/Ce2.5 still retains the nanoplates structure, suggesting the stability of its microstructure. The deactivation might originate from the decrease of pore volume and diameter

Table 2 Catalytic performance of the series of Zn/Al/Ce catalysts[a]

Catalysts	Aniline conversion (%)	MPC yield (%)	Selectivity (%)			
			MPC	NMA	DMA	DPU
Zn/Al/Ce0	91.0	57.6	63.3	10.9	24.3	0.7
Zn/Al/Ce1	94.5	63.1	66.8	7.1	24.9	0.6
Zn/Al/Ce2.5	95.8	78.2	81.6	4.3	13.3	0.4
Zn/Al/Ce5	94.6	72.0	76.1	4.1	18.4	0.7
Zn/Al/Ce7.5	95.6	72.6	75.9	5.3	17.7	0.6
Zn/Al/Ce10	92.6	57.5	62.1	6.6	29.8	0.8

[a] Reaction conditions: DMC 19.35 g, aniline 1 g (molar ratio of DMC to aniline is 25), catalyst 0.253 g, reaction temperature 200 °C, reaction time 7 h.

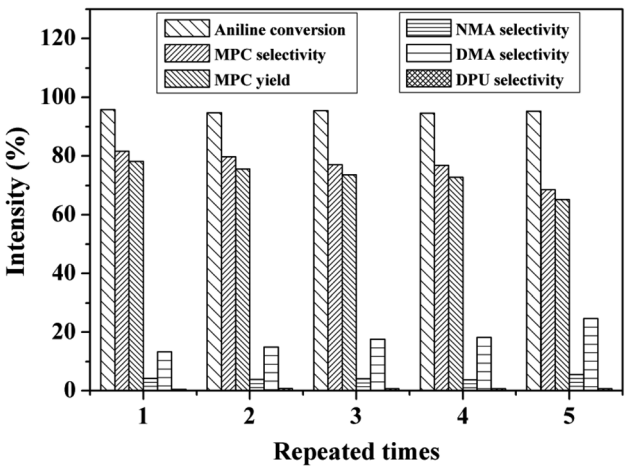

Fig. 5 Recycling test of Zn/Al/Ce2.5. Reaction conditions: molar ratio of DMC to aniline is 25, catalyst 0.253 g, reaction temperature 200 °C, reaction time 7 h.

of catalyst caused by the blocking of organic substances, and the formation of carbonate like species on the surface of catalyst.[25] Moreover, XRD pattern of Zn/Al/Ce2.5 after the cyclic test is almost the same as the uncalcined precursor (Fig. S9†), which confirms the reconstruction of the hydrotalcite structure due to its memory effect.[43] As a result, the catalytic performance of Zn/Al/Ce2.5 may be recovered *via* simple thermal annealing.

The catalytic performance and cycling stability of the present Zn/Al/Ce2.5 are superior to previously reported heterogeneous catalysts, such as $Zn(OAc)_2/SiO_2$,[2] $ZnO–TiO_2$ (ref. 9) and ordered AlSBA-15.[10] As far as we know, there is no report for the reaction of DMC and amine for the synthesis of carbamates (*e.g.* MPC) catalyzed over mixed oxides derived from hydrotalcite-like precursors. Considering the merits of the HTlcs precursors, and the advantages of feasible preparation, low cost, high catalytic performance and stability of the catalyst presented in this preliminary investigation, this kind of catalyst would be promising material for the green synthesis of carbamates. We suspect that the catalytic performance could be further improved *via* optimizing the composition, specific surface area, pore size, and surface acid–base properties, *etc.*

4 Conclusions

In conclusion, herein, we demonstrated the design and fabrication of Zn/Al/Ce mixed oxides as effective and recoverable heterogeneous catalyst for MPC synthesis *via* DMC aminolysis. Zn/Al/Ce hydrotalcite-like precursors and the resulting catalysts were characterized by means of XRD, BET, SEM and XPS, which suggested that strong interactions within the mixed oxides could form *via* the addition of appropriate amount of cerium. Thus, Zn/Al/Ce2.5 showed high DMC aminolysis activity giving aniline conversion of 95.8%, MPC selectivity of 81.6% and MPC yield of 78.2%. Moreover, as a heterogeneous catalyst, Zn/Al/Ce2.5 also exhibited excellent stability for MPC synthesis. This preliminary research provided an alternative and simple method for the developing of high performance heterogeneous catalyst that can be used for the green synthesis of carbamates.

Conflicts of interest

There are no conflicts to declare.

Acknowledgements

We are grateful for grants from Technology Foundation of the Science and Technology Department of Guizhou Province (No. [2017]1208), the Natural Science Research Project of Education Department of Guizhou Province ([2016]093), and Natural Science Foundation of Shanxi Province (No. 201801D121070), Independent Research Project of the State Key Laboratory of Coal Conversion (2018BWZ002).

Notes and references

1 O. Kreye, H. Mutlu and M. A. R. Meier, *Green Chem.*, 2013, **15**, 1431.
2 F. Li, W. Li, J. Li, W. Xue, Y. Wang and X. Zhao, *Appl. Catal., A*, 2014, **475**, 355.
3 B. Han, W. Zhao, X. Qin, Y. Li, Y. Sun and W. Wei, *Catal. Commun.*, 2013, **33**, 38.
4 J. Gao, H. Li, Y. Zhang and W. Fei, *Catal. Today*, 2009, **148**, 378.
5 J. Wang, Q. Li, W. Dong, M. Kang, X. Wang and S. Peng, *Appl. Catal., A*, 2004, **261**, 191.
6 Y. Wang and B. Liu, *Catal. Sci. Technol.*, 2015, **5**, 109.
7 R. Juáreza, H. Pennemann and H. García, *Catal. Today*, 2011, **159**, 25.
8 F. Li, J. Miao, Y. Wang and X. Zhao, *Ind. Eng. Chem. Res.*, 2006, **45**, 4892.
9 F. Li, Y. Wang, W. Xue and X. Zhao, *J. Chem. Technol. Biotechnol.*, 2009, **84**, 48.
10 N. Lucas, A. P. Amrute, K. Palraj, G. V. Shanbhag, A. Vinu and S. B. Halligudi, *J. Mol. Catal. A: Chem.*, 2008, **295**, 29.
11 Y. Pei, H. Li, H. Liu and Y. Zhang, *Catal. Today*, 2009, **148**, 373.
12 F. Qin, Q. Li, J. Wang, Y. Feng, M. Kang, Y. Zhu and X. Wang, *Catal. Lett.*, 2008, **126**, 419.
13 Q. Zhang, H. Yuan, N. Fukaya, H. Yasuda and J.-C. Choi, *Green Chem.*, 2017, **19**, 5614.
14 Q. Zhang, H. Yuan, N. Fukaya and J.-C. Choi, *ACS Sustainable Chem. Eng.*, 2018, **6**, 6675.
15 Z. Zhang, S. Liu, L. Zhang, S. Yin, G. Yang and B. Han, *Chem. Commun.*, 2018, **54**, 4410.
16 S. Laursen, D. Combita, A. B. Hungría, M. Boronat and A. Corma, *Angew. Chem., Int. Ed.*, 2012, **51**, 4190.
17 J. R. Cabrero-Antonino, R. Adam, K. Junge and M. Beller, *Catal. Sci. Technol.*, 2016, **6**, 7956.
18 J. R. Cabrero-Antonino, R. Adam, J. Wärnå, D. Yu. Murzin and M. Beller, *Chem. Eng. J.*, 2018, **351**, 1129.
19 T. Baba, A. Kobayashi, Y. Kawanami, K. Inazu, A. Ishikawa, T. Echizenn, K. Murai, S. Aso and M. Inomata, *Green Chem.*, 2005, **7**, 159.
20 E. Reixach, N. Bonet, F. X. Rius-Ruiz, S. Wershofen and A. Vidal-Ferran, *Ind. Eng. Chem. Res.*, 2010, **49**, 6362.
21 E. Reixach, R. M. Haak, S. Wershofen and A. Vidal-Ferran, *Ind. Eng. Chem. Res.*, 2012, **51**, 16165.
22 X. Zhao, L. Kang, N. Wang, H. An, F. Li and Y. Wang, *Ind. Eng. Chem. Res.*, 2012, **51**, 11335.
23 A. B. Shivarkar, S. P. Gupte and R. V. Chaudhari, *J. Mol. Catal. A: Chem.*, 2004, **223**, 85.
24 D. Sun, S. Xie, J. Deng, C. Huang, E. Ruckenstein and Z. Chao, *Green Chem.*, 2010, **12**, 483.
25 A. Primo, E. Aguado and H. Garcia, *ChemCatChem*, 2013, **5**, 1020.
26 M. Tamura, K. Noro, M. Honda, Y. Nakagawa and K. Tomishige, *Green Chem.*, 2013, **15**, 1567.
27 G. Fan, S. Luo, T. Fang, Q. Wu, G. Song and J. Li, *J. Mol. Catal. A: Chem.*, 2015, **404**, 92.
28 K. A. Alferov, Z. Fu, S. Ye, D. Han, S. Wang, M. Xiao and Y. Meng, *ACS Sustainable Chem. Eng.*, 2019, **7**, 10708.
29 M. Tamura, K. Ito, Y. Nakagawa and K. Tomishige, *J. Catal.*, 2016, **343**, 75.

30 B. Puértolas, M. Rellán-Piñeiro, J. L. Núñez-Rico, A. P. Amrute, A. Vidal-Ferran, N. López, J. Pérez-Ramírez and S. Wershofen, *ACS Catal.*, 2019, **9**, 7708.
31 R. Juárez, P. Concepción, A. Corma, V. Fornés and H. García, *Angew. Chem.*, 2010, **122**, 1308.
32 R. Zhang, L. Guo, C. Chen, J. Chen, A. Chen, X. Zhao, X. Liu, Y. Xiu and Z. Hou, *Catal. Sci. Technol.*, 2015, **5**, 2959.
33 P. Wang, Y. Ma, S. Liu, F. Zhou, B. Yang and Y. Deng, *Green Chem.*, 2015, **17**, 3964.
34 J. Shang, S. Liu, X. Ma, L. Lu and Y. Deng, *Green Chem.*, 2012, **14**, 2899.
35 D. Wang, X. Zhang, X. Cong, S. Liu and D. Zhou, *Appl. Catal., A*, 2018, **555**, 36.
36 P. P. Gao, F. Li, N. Zhao, F. Xiao, W. Wei, L. Zhong and Y. Sun, *Appl. Catal., A*, 2013, **468**, 442.
37 X. Xie, Q. Zhou, X. Hu, X. Jia and L. Huang, *Int. J. Energy Res.*, 2019, **43**, 7075.
38 H. H. Ling, Z. Wang, L. Wang, C. Stampfl, D. Wang, J. Chen and J. Huang, *Catal. Today*, 2019, DOI: 10.1016/j.cattod.2019.01.057.
39 Z. Yan, Z. Xu, J. Yu and M. Jaroniec, *Appl. Catal., B*, 2016, **199**, 458.
40 A. L. Cámara, V. C. Corberán, A. Martínez-Arias, L. Barrio, R. Si, J. C. Hanson and J. A. Rodriguez, *Catal. Today*, 2020, **339**, 24.
41 Q. Li, P. Wang, S. Liu, Y. Fei and Y. Deng, *Green Chem.*, 2016, **18**, 6091.
42 H. Mai, L. Sun, Y. Zhang, R. Si, W. Feng, H. Zhang, H. Liu and C. Yan, *J. Phys. Chem. B*, 2005, **109**, 24380.
43 P. Gao, F. Li, H. J. Zhan, N. Zhao, F. K. Xiao, W. Wei, L. S. Zhong and Y. H. Sun, *Catal. Commun.*, 2014, **50**, 78.

